Macromolecular Research, Vol. 16, No. 6, pp 539-543 (2008)

pH-Triggered Transition of Silk Fibroin from Spherical Micelles to Nanofibrils in Water

Peng Chen, Hyun Suk Kim, Chi-Young Park, Hun-Sik Kim, In-Joo Chin, and Hyoung-Joon Jin*

Department of Polymer Science and Engineering, Inha University, Incheon 402-751, Korea

Received January 11, 2008; Revised February 27, 2008; Accepted March 4, 2008

Abstract: Many natural proteins self-assemble in complex ways, either to fulfill their biological function or introduce particular properties, such as high strength and toughness. We report the morphological transition in water from a spherical to rod-like shape of *Bombyx mori* silk fibroin by reducing the pH. Transmission electron microscopy, scanning electron microscopy, and dynamic light scattering were used to characterize the dilute solutions of silk fibroin in an aqueous environment, and provide direct visualization of the transformation of spherical micelles at pH 6.8 to nanofibrils at pH 4.8. This change in morphology occurred as a result of the stretching entropy due to the formation of β-sheets, which was analyzed using circular dichroism spectroscopy. This study demonstrates the self-assembly of silk fibroin as a function of pH.

Keywords: silk fibroin, nanostructures, self-assembly.

Introduction

Natural silk fibers have been extensively studied, primarily owing to their good mechanical properties, despite being spun at ambient temperatures and pressures while using water as a solvent.[1] However, the spinning process, i.e. the supramolecular structural transition of silk fibroin in the aqueous environment of a gland, remains poorly understood.[2] In efforts to elucidate the processes involved, the self-assembly of many natural proteins such as silk fibroin has been the focal point of a significant body of research over the past few decades, as scientists have strived to discover the fundamental rules of nature and develop new engineering applications.[3,4]

During this time, few results have been reported that clarify the processes involved in the self-assembly of silk fibroin. Inoul *et al.*.[5] reported that silk fibroin from *S. C. ricini* wild silkworm self-assembles to form highly ordered nanofabric structures; however, the effect of the numerous amino acids present in the protein sequence of silk fibroin, including their sensitivity to environmental conditions such as pH and the salt concentration, was not addressed.[6]

One of the most widely studied natural silks is the fibroin that composes fibers from the domestic silkworm *Bombyx mori*.[7] The protein consists primarily of two components, silk fibroin and sericin.[1] In the *B. mori* silkworm, there are two silk glands, each of which is divided into three divisions, namely, the posterior (P), the middle (M), and the anterior (A) divisions. Notably, the pH, salt concentration, and fibroin concentration are controlled in the individual divisions.[8] The middle division is further divided into three parts: the posterior (MP), the middle (MM), and the anterior (MA). Silk fibroin molecules are synthesized within the cells of the P division where they are present in a weak gel state with a concentration of ~12 wt%. This solution is transported to the wider M division, which serves as a reservoir with a fibroin concentration of ~26 wt% present in a stronger gel-like material. This gel-like fibroin begins to undergo a gel-sol transition in the MA division and moves forward to the A division and is stored as a concentrated aqueous solution of ~30 wt%. The two silk glands connect before the spinneret, and at the spinneret, silk fiber is produced from a liquid crystalline solution.[9] The pH is decreased gradually in the lumen of the *B. mori* silkworm from near neutral (pH 6.9) in the posterior division to weakly acidic (pH 4.8) in the anterior division adjacent to the spinneret.[10]

In the present study, the change of the supramolecular structure of silk fibroin from *B. mori* silkworm as a function of pH was characterized. A transition from spherical micelles to nanofibrils was observed in a dilute aqueous solution of the protein with a reduction of the pH. The morphologies were assessed by transmission electron microscopy (TEM) and scanning electron microscopy (SEM) and the results were validated by dynamic light scattering (DLS). Circular dichroism (CD) spectroscopy was used to monitor the secondary structure of the silk fibroin.

*Corresponding Author. E-mail: hjjin@inha.ac.kr

Experimental

Preparation of the Silk Fibroin Aqueous Solution. Cocoons of *B. mori*, kindly provided by Boeun Traditional Sericulture Farm in Korea, were boiled for 20 min in an aqueous solution of 0.02 M Na_2CO_3 and then rinsed thoroughly with distilled water to extract the glue-like sericin proteins. The extracted silk fibroin was then dissolved in a 9.3 M LiBr solution at 60 °C for 4 h, yielding a 20% (w/v) solution. This solution was dialyzed in distilled water using Slide-a-Lyzer dialysis cassettes (molecular weight cutoff, MWCO, 3,500, Pierce) for 2 days. The final concentration of the silk fibroin aqueous solution was about 8 wt%, as determined by weighing the remaining solid after drying.

Acid-Induced Self-Assembly. The fibroin aqueous solution (8 wt%) was kept in vials at 4 °C for 2 weeks to ensure the formation of stable supramolecular assemblies. The pHs of the solutions were adjusted to the desired values by the addition of 0.01 M aqueous hydrochloric acid (HCl). When the pH decreased to 4.4, the sol-gel transition of the silk fibroin aqueous solution occurred immediately. The appearance of cloudiness in the solution indicated that aggregation had taken place. The optical transmission of dilute silk solutions at different pH values was measured by a Turbiscan classic MA2000 (Formulaction, France). For the TEM, SEM, and CD analyses, a concentrated silk fibroin solution was diluted with distilled water to a concentration of 0.5 wt% and the pH was subsequently adjusted with 0.01 M HCl. The pH of the silk solution was monitored with a pH meter (Inolab 720, WTW, USA).

Characterizations. For the TEM analysis, a droplet of silk fibroin solution was deposited directly onto a carbon-coated copper grid and allowed to dry under ambient conditions after immediately wicking away most of the solution. Once dry, the silk fibroin was stained using ca. 2 wt% phosphotungstic acid solution. TEM images of the supramolecular aggregates were obtained in bright-field mode at an accelerating voltage of 120 kV on a Philips CM 200. The silk fibroin was freeze-dried by directly placing it into liquid nitrogen and drying it in a freeze dryer for about 3 days. The samples were prepared by coating them with nano-sized platinum. The morphology of the freeze-dried silk fibroin was observed with FESEM (S-4200SE, Hitachi, Japan). DLS measurements were performed using a Brookhaven BI-200SM goniometer and a BI-9000AT digital autocorrelator at a scattering angle of 90° at room temperature. The light source was a He-Ne laser (632.8 nm). The solutions were filtered through 0.45 μm filters (Whatman Anatop 10). The hydrodynamic diameter (d) of the vesicles was calculated using the Stokes-Einstein equation: $d = k_B T/3\pi\eta D$, where k_B is the Boltzmann constant, T is the absolute temperature, η is the solvent viscosity, and D is the diffusion coefficient. The polydispersity factor of the micelles, represented as μ_2/Γ^2, where μ_2 is the second cumulant of the decay function and Γ is the average characteristic line width, was calculated by the cumulant method.[11,12] The CD spectra of all of the samples at a concentration of 0.5 wt% were recorded on a JASCO J-715 spectrometer at an ambient temperature of 25 °C. A cylindrical quartz cell with a path length of 0.01 cm was used for the spectral measurements. Each spectrum is presented as the average of four consecutive scans measured at a resolution of 0.1 nm.

Results and Discussion

Regenerated silk fibroin solutions (pH 6.8) were prepared based on a procedure described in a previous study[13] and the pH of the solutions was adjusted to the desired value by the addition of 0.01 M HCl. When buffer solutions are used, the rapid aggregation of the silk fibroin does not allow distinct supramolecular assemblies to form and, thus, they are not observed by TEM or SEM. Salt ions in the buffer accelerate the aggregation of the silk fibroin.[14] The dilute silk fibroin solution was found to be soluble and optically transparent at neutral pH, but slow acidification resulted in its precipitation at a pH of less than 4.4. The gelation time of the fibroin solution decreased as the pH of the solution was decreased. Figure 1 shows a photograph of the diluted silk aqueous solutions at both pH 4.8 and 6.8; these two pH levels represent the conditions at different parts of the silk gland of *B. mori.*: pH 4.8 for the anterior division and pH 6.8 for the posterior division. As the pH of the solutions was decreased, their turbidity increased, as shown in Figure 1, indicating the formation of supramolecular structures.[14] In addition, the process of gelation by *B. mori* fibroin, induced by the reduction in pH, took place within several hours, which is much faster than that without the adjustment of the pH value (generally several days is needed), and this process is irreversible.

Micelles have already been identified at neutral pH in a

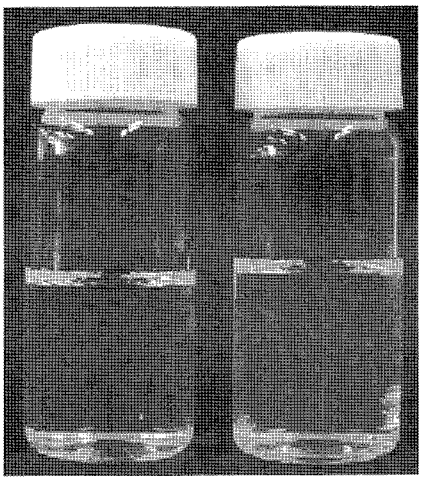

Figure 1. Photographs of dilute silk fibroin aqueous solution (0.5 wt%) at different pHs: (left) pH 6.8 and (right) pH 4.8.

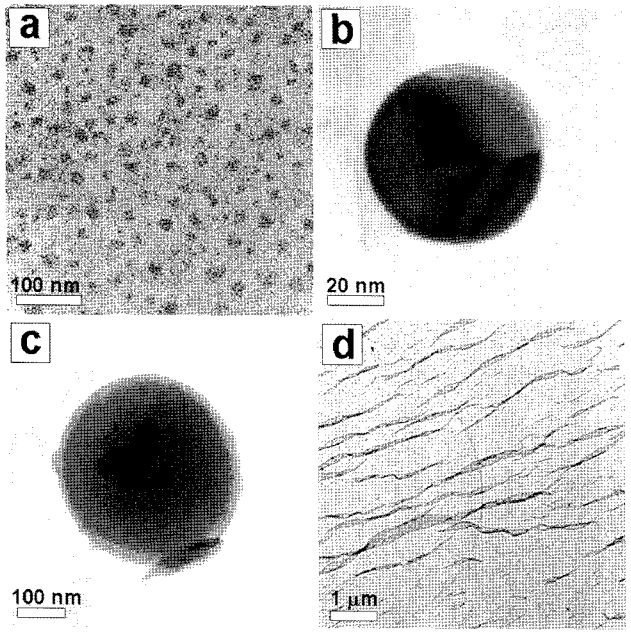

Figure 2. TEM images of regenerated silk fibroin (0.5 wt%) after adjusting the pH to (a, b, c) 6.8 and (d) 4.8.

previous study.[7] In the present study, the observations with dilute silk fibroin solutions imaged by TEM provided more detailed and precise information on the morphology of the micelles with diameters of 20~50 nm (Figure 2(a)). The silk fibroin molecules act as tri-block (hydrophilic-hydrophobic-hydrophilic) copolymers, forming irregular sized micelles, the diameter of which range from several tens of to hundreds of nanometers (Figure 2(b) and Figure 2(c)) depending on the chain folding and hydrophobic interactions (Figure 3).[7] The intervening hydrophilic blocks located among the hydrophobic blocks in the fibroin prevent premature β-sheet formation, thus maintaining the solubility of the fibroin solution.

The SEM image (Figure 4(a)), which was used to verify the observations of the dilute silk fibroin solutions imaged by TEM, provided even more interesting findings. From the SEM image, necklace-like micelles having a diameter of hundreds of nm were observed. This diameter is larger than that observed in the TEM image (i.e., 20~50 nm). This change could be attributed to evaporation through the lengthy drying process. Under the influence of evaporation, a concentration gradient of the unassembled dispersed silk fibroin is created with the concentration increasing from the lower to upper regions. As such, the solvent would be separated out, providing an opportunity for the silk fibroin to be absorbed or to congregate. The adsorption of the dispersed silk fibroin onto the surface of the self-assembled micelles would increase the diameter of the micelles.[15] Synchronously, the agglomeration of the free silk fibroin would also lead to the formation of filaments between pairs of micelles.

In order to visualize the silk fibroin particles in the pristine state under the original solution conditions (pH = 6.8), we employed DLS (Figure 5). Based on the DLS data, the hydrodynamic diameter was determined to be 85 nm, which is also larger than that obtained by TEM (20~50 nm). This discrepancy may due to the greater amount of free space offered in solution, especially at such a low concentration. Accordingly, the protein chain can be more spread out on the surface, which would be conducive to the increase in the diameter of the micelles. In addition, some data indicating the presence of micelles having a diameter exceeding 300 nm was also obtained. This could corroborate the results obtained by TEM (Figure 2(c)), indicting that the diameter depends on the chain folding and hydrophobic interactions.

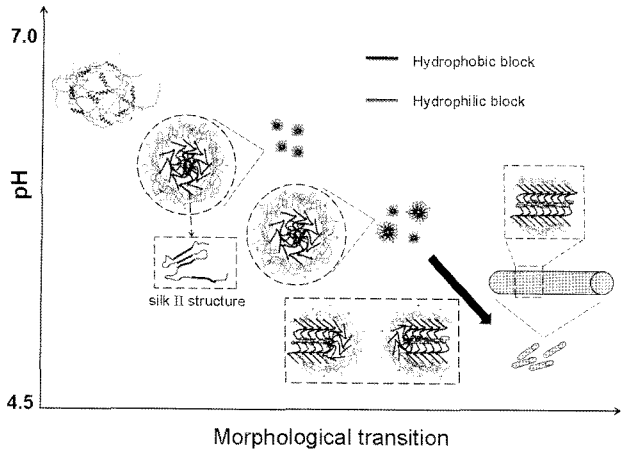

Figure 3. Schematic model of pH-triggered self-assembly of silk fibroin.

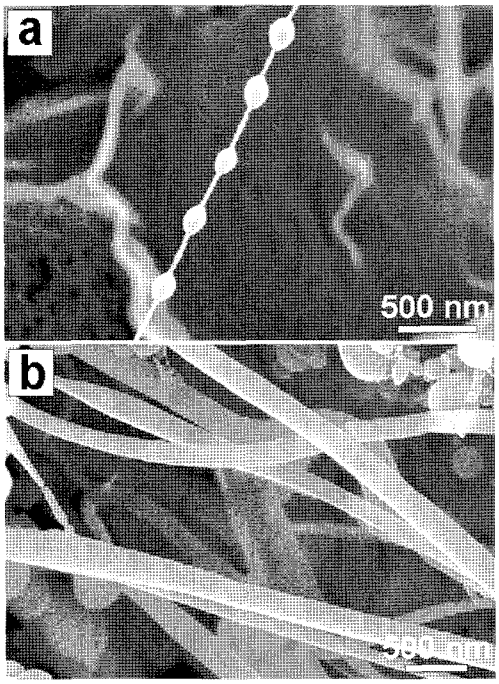

Figure 4. SEM images of regenerated silk fibroin (0.5 wt%) after adjusting the pH to (a) 6.8 and (b) 4.8.

The hydrodynamic diameter is smaller than that found by SEM. This could be explained as follows: At the same concentration of silk fibroin, there would be weaker sorption of the dispersed silk fibroin onto the surface of the micelles in the DLS solution sample than that in the SEM solid sample. Consequently, the main factor influencing the diameter of the micelles would then be the amount of free volume available, and the protein chain could therefore spread out more in the solution. This could explain why the diameter of the micelles, as determined in the DLS analysis, is larger than that obtained by TEM but less than that found by SEM.

Given that some amino acids such as aspartate (1.9%), glutamate (1.4%), arginine (0.5%), and lysine (0.4%) of the larger hydrophilic blocks at the chain-end have charged R groups, it is possible that they might play an important role in the molecular assembly and changes in the secondary structure at a specific pH through electrostatic interactions.[16] Wong Po Foo *et al.* determined the charge distribution and the predicted pI of completely or partially sequenced silk proteins and of the hydrophilic N- and C-termini and the smaller hydrophilic spacer within the hydrophobic domains by ProtParam (ExPASy: Expert Protein Analysis System).[8] The pI of the entire *B. mori* silk fibroin molecules is 3.8-3.9,[17] but the charge distributions and pI values of the hydrophilic C- and N-terminal domains are different (pI: 10.59 for the C-termini, 4.40 for the N-termini). In particular, the light (pI = 5.06) and heavy chains are linked by an intermolecular disulfide bond[18] and the light chains are almost five times as long as the C-terminus of the heavy chain.[19] This allows the overall charge at the C-terminus of the heavy chain to be negative at pH > 5.06. Namely, at neutral pH, both hydrophilic blocks at the chain ends possess a negative charge. The hydrophobic interaction of the internal protein sequence in the fibroin proteins and the electrostatic repulsion of the end blocks induce the formation of spherical micelles with small diameters. The TEM (Figure 2(d)) and SEM (Figure 4(b)) images show that the morphological change of the spherical micelles into nanofibrils occurs when the pH is reduced from 6.8 to 4.8. In the transition step, the net charge of the hydrophilic block containing the L-chain becomes positive at pH 4.8. Therefore, it is reasonable to presume that the reduced electrostatic repulsion between the small spherical micelles leads to the formation of large aggregates of silk fibroin (Figure 2(d) and Figure 4(b)). Furthermore, besides the fibrils, some spherical micelles can also be found, probably because of the limited time. It is reasonable to suppose that a longer time would be required to form the ideal fibrous structure and, consequently, some of the fibroin spherical micelles might not have enough time to finish or even start the conformation transformation and, consequently, they remain as spherical micelles.

The examination of the large aggregates of silk fibroin observed by SEM revealed nanofibrils with diameters of the order of hundreds of nm (Figure 4(b)). Nanofibrils were also formed after the addition of KCl to *Nephila spidroin* solution.[20] Also, *Viney*[21] suggested that orb-weaving spider silks form supramolecular rod-like structures; these structures are assembled extrinsically by the aggregation of the solubilized globular protein chains driven by their amino-acid hydrophobicity. It is clear that the pH is an important factor in the formation of supramolecular assemblies of *B. mori* silk fibroins via its influence on the electrostatic interactions.

Since the morphological transition from spherical micelles to nanofibrils could be explained by the stretching entropy effect of the hydrophobic blocks in the amphiphilic block copolymers,[22] it is necessary to consider the effect of pH on the secondary structure in the hydrophobic block of the silk fibroin molecules. The hydrophobic residues occupy 70% of the silk fibroin sequence. The repetitive sequence in the hydrophobic residues consists of GAGAGS peptides that dominate the β-sheet structure, forming crystalline regions (Silk II) in the silk fibers.[23] Circular dichroism (CD) was used to investigate the effect of the pH on the secondary structure of the silk fibroin. Figure 6 compares the CD spectra of the silk fibroin aqueous solutions at different pHs, measured after adjusting the solutions to the desired pH. The CD results indicate that the conformational transition of the silk fibroin from random coil to β-sheet, a more extended structure, occurs when the pH of the silk fibroin solution is lowered to 4.8.[24] This suggests that the stretching of the hydrophobic blocks in the spherical micelles induced by the β-sheet formation may drive the morphological transition from spherical micelles into nanofibrils. On the basis of the above data, it can be assumed that the hydrophilic blocks of silk fibroin enable this hydrophobic protein to be highly soluble in aqueous solution, while also helping to moderate the morphological change in the supramolecular structures. This process involves the transition from spherical micelles to nanofibrils depending on the pH of the solution. The hydrophobic domains in the silk fibroin facilitate its transition to the fibril-like morphology, driven by the stretching entropy

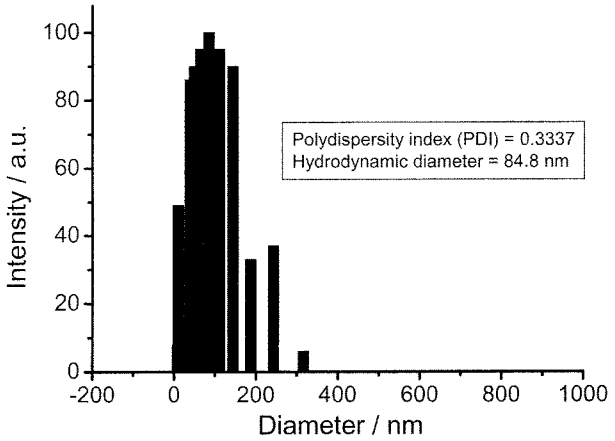

Figure 5. DLS data of regenerated silk fibroin (0.5 wt%) after adjusting the pH to 6.8.

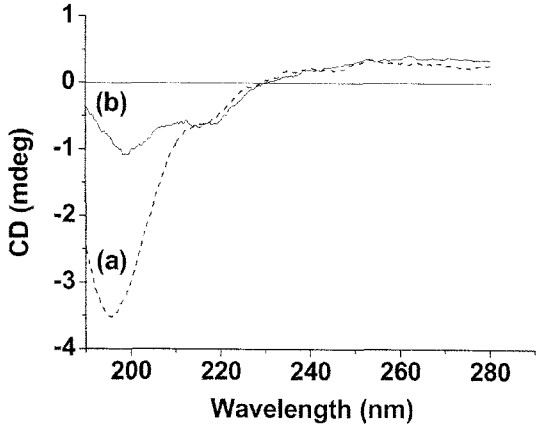

Figure 6. CD spectrum of dilute silk fibroin aqueous solution (0.5 wt%) at different pHs. The pH value of the samples was adjusted to: (a) 6.8 and (b) 4.8.

associated with the increased β-sheet content at pH 4.8.

Conclusions

TEM and SEM characterization provided direct confirmation that silk fibroin in a dilute aqueous solution at pH 6.8 forms spherical micelles with diameters of 20~50 nm. DLS was employed to describe and corroborate the pristine state of these particles in the solution state. Interestingly, at pH 4.8, a morphological transition from spherical micelles to nanofibrils was observed. This transition may be driven by the decreased electrostatic repulsion between the hydrophilic domains at the chain ends of the silkworm fibroin and the stretching entropy effect related to the hydrophobic blocks in the protein. The transition of the secondary structure from random coil to β-sheet during this change in pH from 6.8 to 4.8 was confirmed by CD spectroscopy. These results should shed light on silk processing as well as providing a useful guide for the design of silk and silk-like biomaterials.

Acknowledgements. The authors of this work would like to thank the Korea Science and Engineering Foundation (KOSEF) for sponsoring this research through the SRC/ERC Program of MOST/KOSEF (R11-2005-065).

References

(1) F. Vollrath and D. P. Knight, *Nature*, **410**, 541 (2001).
(2) K. H. Gührs, K. Weisshart, and F. Grosse, *Rev. Mol. Biotechnol.*, **74**, 121 (2000).
(3) Z. Hong, B. Chasan, R. Bansil, B. S. Turner, K. R. Bhaskar, and N. H. Afdhal, *Biomacromolecules*, **6**, 3458 (2005).
(4) E. Oroudjev, J. Soares, S. Arddlacono, J. B. Thompson, S. A. Fossey, and H. G. Hansma, *Proc. Natl. Acad. Sci. USA*, **99**, 6460 (2002).
(5) S. Inoue, H. Tsuda, T. Tanaka, M. Kobayashi, Y. Magoshi, and J. Magoshi, *Nano Lett.*, **3**, 1329 (2003).
(6) C.-Z. Zhou, F. Confalonieri, M. Jacquet, R. Perasso, Z.-G. Li, and J. Janin, *Proteins: Struct., Funct., Genet.*, **44**, 119 (2001).
(7) H.-J. Jin and D. L. Kaplan, *Nature*, **424**, 1057 (2003).
(8) C. Wong Po Foo, E. Bini, J. Hensman, D. P. Knight, R. V. Lewis, and D. L. Kaplan, *Appl. Phys. A*, **82**, 223 (2006).
(9) P. J. Willcox, P. S. Gido, W. Muller, and D. L. Kaplan, *Macromolecules*, **29**, 5106 (1996).
(10) J. Magoshi, Y. Magoshi, M. A. Becker, and S. Nakamura, *ACS National Meeting*, **212**, 53 (1996).
(11) B. Chu, *Laser Light Scattering: Basic Principles and Practice*, 2nd Edition, Academic Press, 1992.
(12) Y. Song, C. Park, and C. Kim, *Macromol. Res.*, **14**, 235 (2006).
(13) U.-J. Kim, J. Park, C. Li, H.-J. Jin, R. Valluzzi, and D. L. Kaplan, *Biomacromolecules*, **5**, 786 (2004).
(14) R. Masui, T. Mikawa, and S. Kuramitsu, *J. Biol. Chem.*, **272**, 27707 (1997).
(15) C. Park, M. Rhue, J. Lim, and C. Kim, *Macromol. Res.*, **15**, 39 (2007).
(16) J. D. Hartgerink, E. Benlash, and S. I. Stupp, *Proc. Natl. Acad. Sci. USA*, **99**, 5133 (2002).
(17) G. D. Kang, J. H. Nahm, J. S. Park, J. Y. Moon, C. S. Cho, and J. H. Yeo, *Macromol. Rapid Commun.*, **21**, 788 (2000).
(18) K. Tanaka, N. Kajiyama, K. Ishikura, S. Waga, A. Kikuchi, K. Ohtomo, T. Takagi, and S. Misuno, *Biochem. Biophys. Acta*, **92**, 1432 (1999).
(19) K. Yamaguchi, Y. Kikuchi, T. Takagi, A. KiKuchi, F. Oyama, K. Shimura, and S. Mizuno, *J. Mol. Biol.*, **210**, 127 (1989).
(20) X. Chen, D. P. Knight, and F. Vollrath, *Biomacromolecules*, **3**, 644 (2002).
(21) F. N. Braun and C. Viney, *Int. J. Bio. Macromol.*, **32**, 59 (2003).
(22) L. Lei, J.-F. Gohy, N. Willet, J.-X. Zhang, S. Varshney, and R. Jérôme, *Macromolecules*, **37**, 1089 (2004).
(23) H. Yamada, H. Nakao, Y. Takasu, and K. Tsubouchi, *Mater. Sci. Eng. C*, **14**, 41 (2001).
(24) Y. Yang, Z. Shao, X. Chen, and P. Zhou, *Biomacromolecules*, **5**, 773 (2004).